1521-009X/41/12/2081–2086$25.00
Drug Metabolism and Disposition

http://dx.doi.org/10.1124/dmd.113.053736
Drug Metab Dispos 41:2081–2086, December 2013

N-Acetylation of Etamicastat, a Reversible Dopamine-β-Hydroxylase Inhibitor

Ana I. Loureiro, Carlos Fernandes-Lopes, Maria João Bonifácio, Lyndon C. Wright, and Patrício Soares-da-Silva

Department of Research and Development, BIAL – Portela & C[a], S.A., S. Mamede do Coronado, Portugal, (A.I.L., C.F.-L., M.J.B., L.C.W, P.S.d.S.); and Faculty of Medicine, Institute of Pharmacology and Therapeutics, Porto, Portugal (P.S.d.S.)

Received July 16, 2013; accepted September 6, 2013

ABSTRACT

Etamicastat [(*R*)-5-(2-aminoethyl)-1-(6,8-difluorochroman-3-yl)-1*H*-imidazole-2(3*H*)-thione hydrochloride] is a reversible dopamine-β-hydroxylase inhibitor that decreases norepinephrine levels in sympathetically innervated tissues. After in vivo administration, *N*-acetylation of etamicastat was found to be a main metabolic pathway. The purpose of the current study was to characterize the *N*-acetylation of etamicastat by *N*-acetyltransferases (NAT1 and NAT2) and evaluate potential species differences in etamicastat *N*-acetylation using a sensitive and specific liquid chromatography–mass spectrometry assay. Marked differences in etamicastat *N*-acetylation were observed among the laboratory species and humans. After oral administration, the rat, hamster, and human subjects presented the highest rates of etamicastat *N*-acetylation, whereas almost no acetylation was observed in the mouse, rabbit, minipig, and monkey and no acetylation was observed in the dog. In in vitro studies, rats and humans showed similar acetylation rates, whereas no acetylation was detected in the dog. Studies performed with human recombinant NAT1 4 and NAT2 4 enzymes revealed that both were able to conjugate etamicastat, although at different rates. NAT1 had lower affinity compared with NAT2 (K_m, 124.8 ± 9.031 μM and 17.14 ± 3.577 μM, respectively). A significant correlation (r^2 = 0.65, P < 0.05) was observed in a comparison of etamicastat *N*-acetylation by human single-donor enzymes and sulfamethazine, a selective substrate to NAT2. No correlation was observed with *p*-aminosalicylic acid, a NAT1 selective substrate. In conclusion, these results suggest that NAT2 and, to a lesser extent, NAT1 contribute to etamicastat *N*-acetylation. Furthermore, the high interspecies and intraspecies differences in *N*-acetylation should be taken into consideration when evaluating the in vivo bioavailability of etamicastat.

Introduction

N-Acetyltransferase (NAT) is one of the major hepatic phase II enzymes involved in drug metabolism. NAT, a cytosolic protein that is expressed in a wide variety of tissues, plays an important role in the *N*-acetylation of drugs containing aromatic amine and hydrazine groups, converting them to aromatic amides and hydrazides, respectively.

Humans express two functional NAT isoforms, NAT1 and NAT2. NAT1 is widely distributed in the organism, whereas NAT2 has a restricted tissue distribution with higher levels of expression in the liver and intestine (Meyer, 1994; Husain et al., 2007). *N*-acetyltransferases exhibit different substrate specificities; in humans, isoniazid and sulfamethazine are efficiently *N*-acetylated by NAT2, whereas *p*-aminobenzoic acid is a substrate for NAT1 (Meyer, 1994; Stevens et al., 1999). It is recognized that human NAT1 and NAT2 loci are highly polymorphic, with more than 25 alleles identified in each locus (Hein et al., 2000a,b; Stanley and Sim, 2008; Walraven et al., 2008). As an important metabolizing enzyme in humans, the polymorphisms in human NAT expression, especially NAT2, raise concerns about drug–drug interactions related to drug metabolism during clinical use (Spielberg, 1996; Dorne, 2004). Slow and rapid acetylators of both forms of NAT1 and NAT2 were identified in humans (Grant et al., 1991; Meyer, 1994). In addition to NAT polymorphisms, species differences in drug *N*-acetylation were also described (Glinsukon et al., 1975; Sharer et al., 1995; Gao et al., 2006), which could introduce interspecies variability in drug metabolism, raising concerns about the use of certain animal species for metabolic profiling of new compounds.

Etamicastat [(*R*)-5-(2-aminoethyl)-1-(6,8-difluorochroman-3-yl)-1*H*-imidazole-2(3*H*)-thione hydrochloride; also known as BIA 5-453] is a novel peripheral selective dopamine-β-hydroxylase inhibitor being developed by BIAL – Portela & C[a], S.A. (S. Mamede do Coronado, Portugal) as a new putative drug therapy for cardiovascular disorders (Fig. 1). Etamicastat acts mainly at the periphery by decreasing noradrenaline levels in sympathetically innervated tissues (Bonifácio et al., 2009) and reduces both systolic blood pressure and diastolic blood pressure, alone or in combination with other antihypertensive drugs, as well as noradrenaline urinary excretion in spontaneously hypertensive rats (Igreja et al., 2008, 2011), with no significant changes in heart rate. In humans, etamicastat was well tolerated after single oral doses (range, 2–1200 mg) (Rocha et al., 2011) and multiple once-daily oral doses (range, 25–600 mg) (Nunes et al., 2010). Studies of etamicastat in healthy subjects showed extensive *N*-acetylation of etamicastat to the inactive metabolite BIA 5-961, as well as, large interindividual variability in pharmacokinetic parameters of both etamicastat and BIA 5-961 (Nunes et al., 2010, 2011; Rocha et al., 2011; Vaz-da-Silva et al., 2011). A pharmacogenetic investigation showed that such variability was dependent upon differences in individual NAT2 genotypes (e.g., single

This study was supported by BIAL – Portela & C[a], S.A.
dx.doi.org/10.1124/dmd.113.053736.

ABBREVIATIONS: BIA 5-961, (*R*)-*N*-(2-(1-(6,8-difluorochroman-3-yl)-2-thioxo-2,3-dihydro-1*H*-imidazol-5-yl)ethyl)acetamide; LC/MS, liquid chromatography–mass spectrometry; NAT, *N*-acetyltransferase.

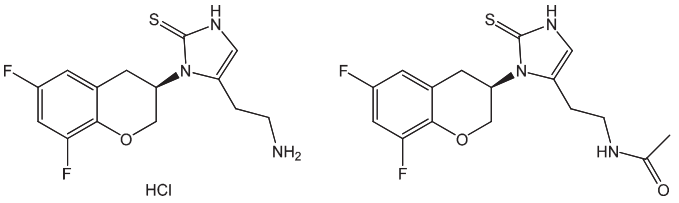

Fig. 1. Structural formula of etamicastat and its *N*-acetylated metabolite BIA 5-961.

nucleotide polymorphisms) evaluated by polymerase chain reaction/restriction fragment length polymorphism analysis (Cascorbi et al., 1995), leading to phenotypic differences in *N*-acetylation metabolizing ability (i.e., rapid or poor acetylator status) (Nunes et al., 2010, 2011; Rocha et al., 2011; Vaz-da-Silva et al., 2011).

This study aimed to characterize both the potential interspecies differences in *N*-acetylation of etamicastat as well as the role of NAT1 and NAT2 in *N*-acetylation of etamicastat.

Materials and Methods

Chemicals. Etamicastat and *N*-acetylated etamicastat [BIA 5-961: (*R*)-*N*-(2-(1-(6,8-difluorochroman-3-yl)-2-thioxo-2,3-dihydro-1*H*-imidazol-5-yl)ethyl) acetamide] were synthesized in the BIAL Laboratory of Chemistry (S. Mamede Coronado, Portugal), with purities >95%. All other chemicals were purchased from Sigma-Aldrich (St. Louis, MO).

Recombinant human arylamine *N*-acetyltransferase 1 4 wild-type allele (NAT1) and arylamine *N*-acetyltransferase 2 4 wild-type allele (NAT2) expressed in baculovirus-infected insect cells were purchased from BD Gentest (Woburn, MA). Pooled human, monkey, dog, and rat liver S9, cytosolic fraction, and cytosolic fraction from single donors (HH18, HH31, HH35, HG42, and HH47) were purchased from BD Gentest. The protein contents were used as described in the data sheets provided by the manufacturers.

Laboratory Animals. Adult male Wistar rats (150–200 g body weight), CD1 mice (20–25 g body weight), and Syrian hamsters (85–130 g body weight), supplied by Harlan (Barcelona, Spain), were kept 5 per cage under controlled environmental conditions (12-hour light/dark cycle; room temperature, 22°C ± 1°C; humidity, 50% ± 5%) with free access to food and tap water.

Female Himalayan rabbits (2.22–3.17 kg body weight), supplied by Charles River Germany (Kisslegg, Germany), were kept individually in stainless steel cages under continuously monitored environmental conditions (room temperature, 18°C ± 3°C; relative humidity, 30%–70%), with a 12-hour fluorescent light/12-hour dark cycle with music during the light period. Pelleted standard food was available ad libitum.

Male and female (nonpregnant) Göttingen SFP minipigs (males, 19–20 kg body weight; females, 14–15 kg body weight), supplied by Ellegard Göttingen Minipigs ApS (Dalmose, Denmark), were housed in individual pens under continuously monitored environmental conditions (room temperature, 20°C–23°C; relative humidity, 30%–70%), with a 12-hour fluorescent light/12-hour dark cycle. Animals were given 400 g pelleted pig diet presented twice daily.

Male and female (nulliparous and nonpregnant) Cynomolgus monkey (*Macaca fascicularis*) (males, 2.11–2.52 kg body weight; females, 1.86–2.24 kg body weight), supplied by Harlan Laboratories SrL (Milan, Italy), were housed in group cages. Each cage housed animals of the same sex under continuously monitored environmental conditions (room temperature, 20°C–24°C; relative humidity, 40%–70%), with a 12-hour fluorescent light/12-hour dark cycle. Each animal was given 180 g/d pelleted standard monkey diet.

All animal procedures were conducted in strict adherence to the European Directive for Protection of Vertebrate Animals Used for Experimental and Other Scientific Purposes (86/609CEE), Portuguese legislation, and the rules of the Guide for the Care and Use of Laboratory Animals (7th edition, 1996). The number of animals used was the minimum possible in compliance with current regulations and scientific integrity.

Human Subjects. Young human healthy volunteers were enrolled in the study while participating in a single-center, entry-into-humans, phase 1, double-blind, randomized placebo-controlled study as previously described (Rocha et al., 2011). Etamicastat (1200 mg) was administered with 250 ml water, in the morning, after an overnight fast and subjects remained fasted at least 4 hours postdose. A normal sodium diet (NaCl = 7 g/d) was provided and no concomitant medication was allowed during the study. The clinical part of the study was conducted in accordance with the principles of the Declaration of Helsinki as well as Good Clinical Practice Guidelines. An independent ethics committee (CCP Ouest VI, Brest, France) reviewed and approved the study protocol and the subject information. Written informed consent was obtained for each subject prior to enrollment in the study.

Sample Handling. Animals were fasted the night before administration. Etamicastat (mice, hamster, and rat, 100 mg/kg; dog, 20 mg/kg; rabbit, 60 mg/kg; minipig, 120 mg/kg; monkey, 75 mg/kg) was given orally (p.o.) as a solution in water. Blank plasma was obtained from animals not subject to any treatment. In the experiments designed to evaluate in vivo etamicastat *N*-acetylation, samples were collected from anesthetized dogs, mice, hamsters, and rats at 3 and 9 hours postdosing and from anesthetized rabbits, minipigs, and monkeys at 2 and 24 hours postdosing. Human samples were collected at 2- and 24- hour time points for comparison with the laboratory animals. Blood was collected and kept on ice until centrifuged at 1500 × *g* for 10 minutes at 4°C. We added 100 μl acetonitrile containing a concentration of 500 ng/ml internal standard to a 100 μl aliquot of plasma. After protein precipitation at room temperature, plasma samples were filtered using a 0.2-μm filter and samples were then injected into liquid chromatography–mass spectrometry (LC/MS).

Etamicastat *N*-Acetylation In Vitro by Different Species. Briefly, *N*-acetylation by human, monkey, dog, and rat S9 fraction and pooled human cytosol was measured using an incubation mixture (100 μl total volume) containing 2 mg/ml total protein, 5 mM $MgCl_2$ and 0.25 mM acetyl-CoA in 50 mM phosphate buffer (pH 7.5). After 5 minutes, preincubation reactions were initiated with 10 μM etamicastat. Reaction mixtures were incubated for up to 60 minutes and terminated with 100 μl 1% formic acid in acetonitrile. All incubations were performed in a shaking water bath at 37°C. After removal of the protein precipitates by centrifugation for 10 minutes at 15,000 × *g*, the supernatant was filtered through 0.2-μm Spin-X filters (Corning Incorporated, Corning, NY) and injected into LC-MS.

Kinetics of Etamicastat *N*-Acetylation in Human Pooled Cytosol. *N*-acetylation rates were determined in human pooled cytosol as described above, with etamicastat concentrations ranging from 5 to 500 μM. Experimental assay conditions for the determination of *N*-acetylation rates in human pooled cytosol were previously optimized by evaluating time (0–120 minutes) and protein dependency (0.5– 3 mg/ml) of the enzymatic assay. Reactions were then carried out with 2 mg/ml total protein and an incubation time of 15 minutes. The reaction was terminated by adding ice-cold acetonitrile 1% formic acid. After precipitation, the samples were vortexed and centrifuged and supernatants were filtered through Spin-X filters (0.2 μm; Costar). The supernatant was injected into LC-MS.

Etamicastat In Vitro *N*-Acetylation by Human Single-Donor Cytosolic Fraction. *N*-acetylation by the human single-donor cytosolic fraction was measured using the above-described conditions. After preincubation with cytosol from single donors, the reaction was initiated by adding 500 μM etamicastat and the mixture was incubated for up to 15 minutes.

Kinetics of Etamicastat *N*-Acetylation by NAT1 and NAT2. The acetylating reaction for recombinant NAT1 and NAT2 fractions was performed in duplicate in a final reaction volume of 100 μl, consisting of 0.1 mM acetyl-CoA, an acetyl-CoA regenerating system composed of 5 mM acetyl-DL-carnitine and 1 unit of carnitine acetyltransferase per milliliter of assay buffer (250 mM triethanolamine-HCl, 5 mM dithiothreitol, pH 7.5) and NAT1 and NAT2 at the concentration of 0.04 μg/ml. The rate of *N*-acetylation was determined with etamicastat concentrations ranging from 5 to 250 μM and 5 to 2000 μM, for NAT2 and NAT1, respectively. The reaction was terminated by adding ice-cold acetonitrile 1% formic acid. After precipitation, the samples were vortexed and centrifuged and supernatants were filtered through Spin-X filters (0.2 μm; Costar). The supernatant was injected into LC-MS. The reaction was evaluated for the linearity of the product formation with respect to the incubation time (0–60 minutes) and to protein concentration (0.1–10 μg/ml).

LC-MS Analysis. Analysis of the extracted plasma samples was performed using liquid chromatography coupled to tandem mass spectrometry (Quattro Ultima; Waters, Milford, MA) with positive (etamicastat) and negative (BIA 5-961) ion detection. Separation was performed on a Symmetry C8 column (3.5 μm,

0.46 cm × 15 cm; Waters) using water/acetonitrile 0.1% formic acid (20:80, v/v) as the mobile phase. Electrospray ionization was used with a capillary current of 2.8 kV. The multiple reaction monitoring pairs were as follows: *m/z* 312→283, collision of 25 eV, and cone voltage of 25 V for etamicastat; *m/z* 352→184, collision of 30 eV, and cone voltage of 30 V for BIA 5-961; and *m/z* 402→120, collision of 25 eV, and cone voltage of 25 V for the internal standard, an etamicastat similar molecule, BIAL's proprietary compound. The analysis of samples extracts from in vitro studies was performed using LC-MS (atmospheric pressure-electrospray ionization, 1100 Series; Agilent Technologies, Santa Clara, CA) with negative ion detection. Separation was performed on a Zorbax SB-C_{18} column (3 μm, 30 × 4.6 mm; Agilent) using a mobile phase A (water containing 0.1% formic acid v/v) and a mobile phase B (methanol containing 0.1% formic acid v/v), with isocratic conditions of 50% of A and 50% of B. Selected by monitoring with the detection of *m/z* of 352 was used for BIA 5-961 quantification. For maximal sensitivity, the fragment energy was set to 120 V and further settings were 3500 eV for capillary voltage, 350°C for nebulizer gas temperature, and 40 psi for nebulizer pressure.

Data Analysis. Kinetic parameters of etamicastat *N*-acetylation were obtained by fitting velocity data using GraphPad Prism software (GraphPad Software, Inc., La Jolla, CA) and the Michaelis-Menten (Eq. 1) and Houston and Kenworthy (Eq. 2) equations as shown below:

$$v = \frac{V_{max} \cdot S}{K_m + S} \quad (1)$$

where v is the rate of the reaction, V_{max} is the maximum velocity, K_m is the Michaelis constant, and S is the substrate concentration; and

$$v = \frac{V_{max} \cdot S}{K_m + S + \left(\frac{S^2}{K_{si}}\right)} \quad (2)$$

where K_{si} is the constant describing the substrate inhibition interaction. All data are reported as the mean ± S.E.M.

Results

Etamicastat N-Acetylation in Laboratory Animals and Humans. Upon oral administration, the levels of etamicastat and its *N*-acetylated metabolite were quantified in the rat, mouse, hamster, rabbit, dog, minipig, monkey, and human plasma at two time points (Fig. 2). The circulating levels of etamicastat and its *N*-acetylated metabolite were markedly different across species. In the dog, only etamicastat could be detected at 3 and 9 hours after oral administration of the parent compound. In the mouse, rabbit, minipig, and monkey, plasma levels of the *N*-acetylated metabolite of etamicastat (BIA 5-961) were considerably lower than that of the parent compound. The highest levels of *N*-acetylated etamicastat were detected in the rat, hamster, and human healthy volunteers, comprising between 40% and 63% of the

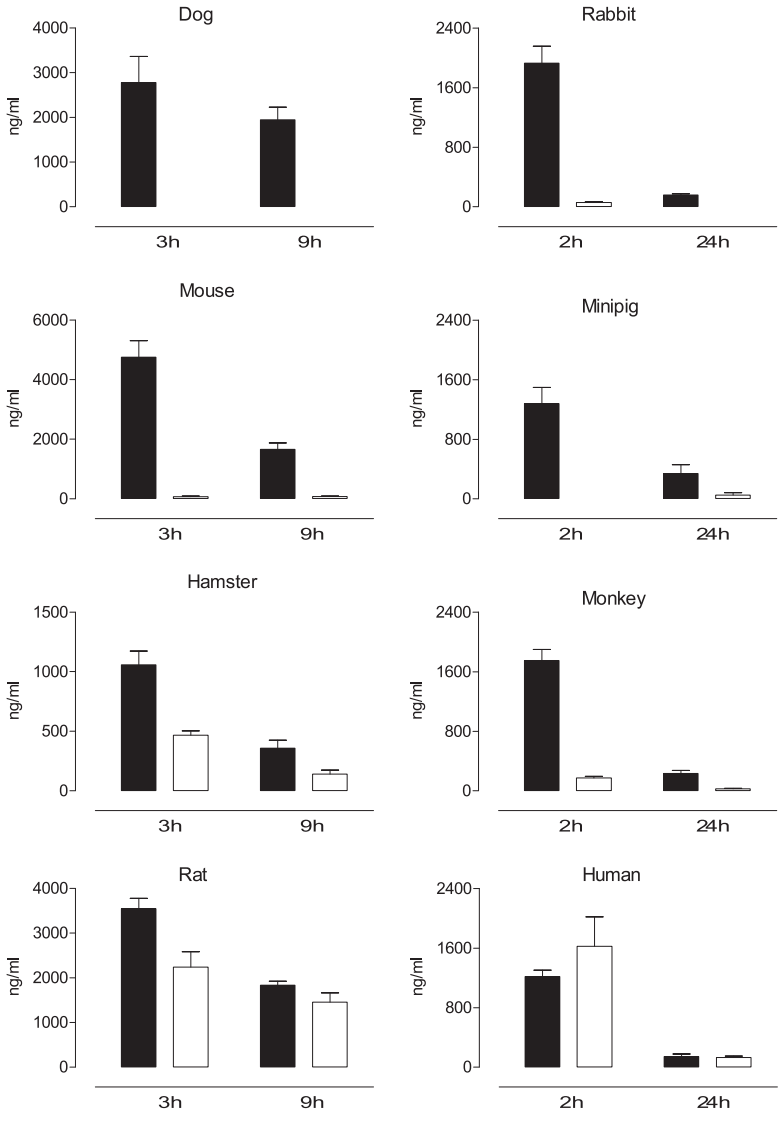

Fig. 2. Mean plasma etamicastat (closed bars) and *N*-acetylated etamicastat (open bars) in dog, rabbit, mouse, minipig, hamster, monkey, rat, and young healthy humans after *p.o.* administration of etamicastat (mice, hamsters, and rats, 100 mg/kg; dog, 20 mg/kg; rabbit, 60 mg/kg; minipig, 120 mg/kg; monkey, 75 mg/kg; humans, 1200 mg). Columns represent mean values and vertical lines indicate the S.E.M. of 3–14 subjects per group.

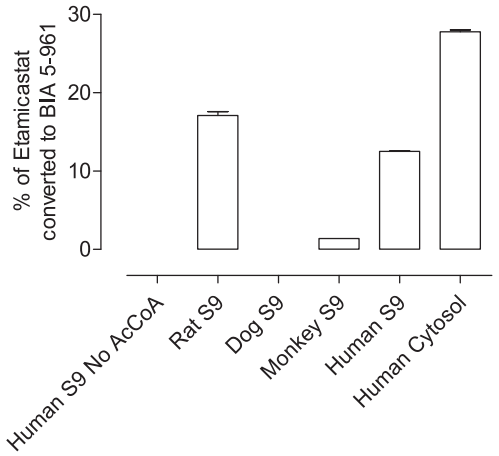

Fig. 3. Etamicastat *N*-acetylation by liver S9 from rat, dog, and monkey and by human S9 and cytosol pools. Etamicastat concentration was 500 μM. Values represent the mean ± S.E.M. of duplicates.

circulating etamicastat in hamsters and rats, respectively. In humans, similar levels of etamicastat and its *N*-acetylated metabolites were detected at 2 and 24 hours postdosing.

Etamicastat *N*-Acetylation by Different Species In Vitro. To evaluate the in vitro *N*-acetylation by different species, etamicastat was incubated with liver enzymes from rat, dog, monkey, and humans with and without acetyl-CoA, a necessary cofactor for NAT activity. As shown in Fig. 3, no *N*-acetylation of etamicastat was detected in the absence of acetyl-CoA. In the presence of acetyl-CoA, there were marked interspecies differences in etamicastat *N*-acetylation. *N*-acetylated etamicastat was detected in human, rat, and monkey, but the levels of *N*-acetylated compound in the monkey were less than one-tenth of those in the rat and in humans. No *N*-acetylation of etamicastat was observed in the dog.

Etamicastat *N*-Acetylation by Human Cytosol. Kinetic analysis of etamicastat *N*-acetylation was performed in human liver cytosolic fraction pools. As shown in Fig. 4, preparations displayed typical hyperbolic kinetics. The apparent kinetic parameters derived from the curve fitted to the Michaelis-Menten equation are listed in Table 1. The intrinsic clearance ($Cl_{int} = V_{max}/K_m$) of etamicastat in human liver cytosolic fraction pools was 0.127 μl/mg protein^{-1} per min^{-1}.

Interindividual Differences in Etamicastat *N*-Acetylation. *N*-acetylation of etamicastat was measured in the cytosolic fractions from five (NAT1) or four (NAT2) human donors (HH18, HH31, HH35, HG42, and HH47) chosen to provide differences in their catalytic activities of the NAT1 and NAT2 enzymes (Table 2). As shown in Fig. 5, the *N*-acetylation rate of etamicastat was different for the different donors. No positive correlation was obtained between etamicastat *N*-acetylation by human liver cytosol single donors and NAT1 activity against the NAT1 typical substrate *p*-aminosalicylic acid. In contrast, a significant correlation ($r^2 = 0.65$, $P < 0.05$) was obtained between the *N*-acetylation rate of etamicastat and that of sulfamethazine, a NAT2 typical substrate (Fig. 6).

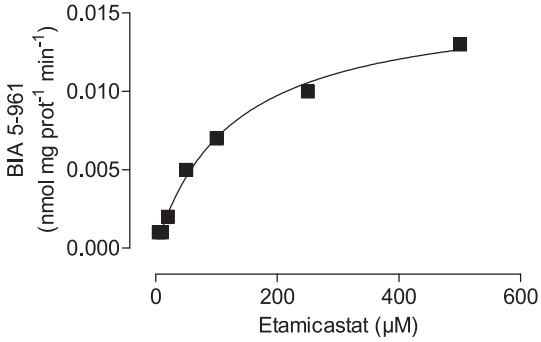

Fig. 4. Kinetics of etamicastat *N*-acetylation by human liver cytosol. Etamicastat concentrations ranged from 1 to 500 μM. Values represent the mean ± S.E.M. of duplicates. Lines represent the fitting curves to the Michaelis-Menten equation as described in *Materials and Methods*.

TABLE 1

Apparent kinetic parameters of etamicastat *N*-acetylation in human liver cytosol and recombinant NAT enzymes

Values represent best-fit values ± S.E.M.

Source of NAT	K_m	V_{max}
	μM	*pmol/mg protein*$^{-1}$ *per min*$^{-1}$
Human cytosol[a]	124.8 ± 9.031	15.8 ± 0.432
NAT1[b]	3399 ± 312.0	1.50 ± 0.0995
NAT2[b]	17.14 ± 3.577	0.810 ± 0.0874

Rates were fitted to the Michaelis-Menten equation (human cytosol, NAT1) and the substrate inhibition equation (NAT2). The K_{si} value obtained was 161.7 ± 36.3.
[a]0.25 mM acetyl-CoA.
[b]0.1 mM acetyl-CoA.

Kinetics of Etamicastat *N*-Acetylation by Recombinant NAT. The characterization of the kinetics of etamicastat *N*-acetylation was performed for both NAT1 and NAT2. Each enzyme was incubated with different concentrations of etamicastat (5–250 μM to NAT2 and 5–2000 μM to NAT1) and the initial rates were determined. The experimental data from NAT1 were fitted with the Michaelis-Menten equation. The data obtained from NAT2, showing an obvious substrate inhibition profile, were fitted with the Houston and Kenworthy equation. The resulting curves are shown in Fig. 7 and the apparent kinetic parameters K_m and V_{max} derived from these curves are depicted in Table 1. The enzyme with the highest affinity for the *N*-acetylation was NAT2, with a K_m of 17.14 ± 3.577 μM. NAT1 had lower apparent affinity, with a K_m of a 3399 ± 312.0 μM. Accordingly, it is possible to assume that NAT2 is the most important enzyme involved in the conjugation of etamicastat in the liver, since NAT1 has much lower affinity.

Discussion

Etamicastat is a reversible dopamine-β-hydroxylase inhibitor that undergoes *N*-acetylation in humans that is markedly influenced by the NAT phenotype. NAT *N*-acetylation is mainly described for drugs containing aromatic amine and hydrazine groups; etamicastat, although not containing any of these groups, was shown to be highly *N*-acetylated in the aminoethyl group (Nunes et al., 2010). Therefore, a full understanding of the contribution of NATs enzymes in etamicastat *N*-acetylation is essential for the evaluation of the interindividual variability of etamicastat and its acetylated metabolite observed in clinical trials (Rocha et al., 2011).

In this study, the kinetic parameters for etamicastat *N*-acetylation by recombinant NATs were determined and compared with those

TABLE 2

Activities of NATs in single-donor human liver cytosol

Data are from BD Biosciences.

Recombinant enzyme	Assay	HH18	HH31	HH35	HG42	HH47
		pmol/mg protein^{-1} *per min*$^{-1}$				
NAT1	*p*-Aminosalicylic acid	60	23	220	430	120/700
NAT2	Sulfamethazine	270	520	500	200	50/10

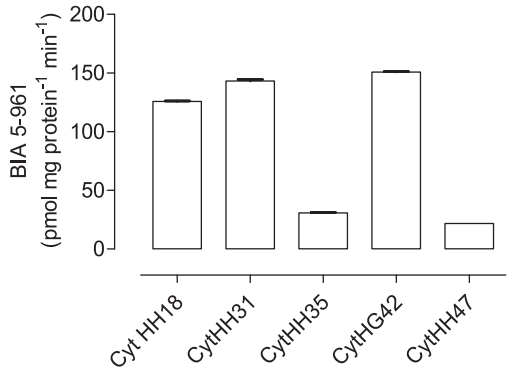

Fig. 5. Etamicastat *N*-acetylation by cytosolic fractions from different donors. Liver cytosol from four to five donors (HH18, HH31, HH35, HG42, and HH47) was incubated with 500 μM etamicastat for 15 minutes at 37°C. Values represent the mean ± S.E.M. of duplicates.

obtained with human liver cytosol in an attempt to elucidate which enzymes contribute to etamicastat *N*-acetylation in vivo. *N*-acetylation of etamicastat in different species and human intraindividual *N*-acetylation variability were also evaluated using in vitro and in vivo experimental models.

The results revealed marked differences in etamicastat *N*-acetylation among the species studied. The rat, hamster, and human species showing the highest etamicastat *N*-acetylation rates, whereas mice, rabbit, minipig, and monkey had almost no acetylated derivative, which accounted to less than 5% of the parent compound. *N*-acetylation of etamicastat in the hamster and rat accounts for approximately 40% and

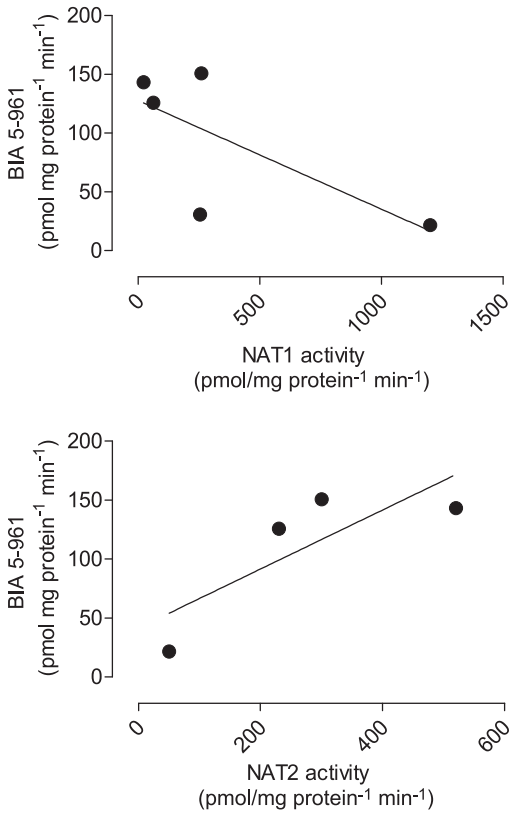

Fig. 6. Relationship between *N*-acetylated etamicastat and sulfamethazine NAT activity, a selective substrate to NAT2, and *p*-aminosalicylic acid, a selective substrate for NAT1. Liver cytosol from four donors was incubated with 500 μM etamicastat for 15 minutes at 37°C. Values represent the mean ± S.E.M. of duplicates.

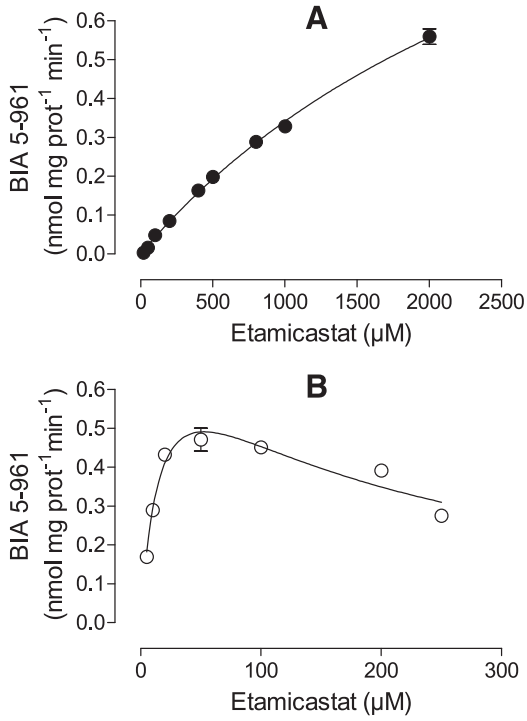

Fig. 7. Kinetics of etamicastat *N*-acetylation by recombinant human NAT enzymes. Etamicastat concentrations ranged from 5 to 2000 μM for NAT1 (A) and from 5 to 250 μM for NAT2 (B). Values represent the mean ± S.E.M. of duplicates. Lines represent the fitting curves as described in *Materials and Methods*.

63% of the parent compound, respectively. In humans, levels of the *N*-acetylated metabolite were similar to those of circulating etamicastat. These data suggest differences in etamicastat pharmacokinetics, metabolism, and/or absorption among species. The levels of etamicastat in circulation may depend on the relative rate of *N*-acetylation, the route and the amount of etamicastat absorbed and excreted, and the extent of other metabolic pathways. In agreement with the in vivo studies, the in vitro studies showed different etamicastat *N*-acetylation profiles among rats, dogs, monkeys, and humans. With exception of dogs, etamicastat N-acetylation was observed in all species examined. The extent of N-acetylation was similar in rat and human S9 fractions and minor in monkeys. The *N*-acetylation pathway of etamicastat was absent in dogs, because NATs are not expressed in this species (Otsuka et al., 1983; Sharer et al., 1995; Savidge et al., 1998; Gao et al., 2006). The substantial differences in etamicastat *N*-acetylation observed between species were expected, since species differences and polymorphisms were previously observed in NAT expression (Gao et al., 2006). In addition, previous studies reported that different factors, including genetic variation, age, sex, and tissue type, may alter NAT activity in mice, Syrian hamsters, and humans (Levy et al., 1992; Estrada et al., 2000). Furthermore, although rats, humans, and monkeys express NAT, the relative expression and activity levels could affect etamicastat metabolism, resulting in interspecies differences. Interspecies scaling is often used to estimate the appropriated dosage for humans, based on the pharmacokinetics of drugs in animals (Mahmood et al., 2003). For etamicastat, however, the differences in *N*-acetylation between species could affect the accuracy of this approach. Moreover, the known genetic polymorphism of human NAT suggests that caution must be taken due to interindividual variability (Hein et al., 2000a,b; Sugamori et al., 2003; Stanley and Sim, 2008).

To characterize in vitro *N*-acetylation of etamicastat, pooled human cytosol and recombinant NATs were used. Pooled human liver cytosol

N-acetylates etamicastat, with a K_m 124.8 ± 9.0 μM and an intrinsic clearance of 0.127 μl/mg protein^{-1} per min^{-1}. Studies performed with human NAT1 4 and NAT2 4 showed that both enzymes were able to conjugate etamicastat albeit at different rates. NAT1 4 is a low-affinity enzyme with a K_m of 3399 ± 312.0 μM for etamicastat *N*-acetylation, whereas NAT2 4 is a high-affinity enzyme with a K_m of 17.14 ± 3.577 μM. In addition, the *N*-acetylation by cytosolic fraction from individual donors with different NAT1 and NAT2 activity correlates well with sulfamethazine *N*-acetylation, a selective substrate to NAT2, but not with *p*-aminosalicylic acid, a selective substrate to NAT1. These results thus suggest that etamicastat *N*-acetylation is primarily produced through NAT2. In fact, a previous study showed that the high interindividual variability in etamicastat *N*-acetylation observed in subjects included in clinical trials was attributed to a different NAT2 phenotype evaluated by polymerase chain reaction/restriction fragment length polymorphism analysis (Rocha et al., 2011). Slow acetylator status may predispose patients to excessive pharmacological effects of etamicastat by allowing more parent drug to be available.

N-acetylation has been suggested to be the primary route of etamicastat biotransformation and the results obtained herein extend our understanding of etamicastat metabolism. NAT2 is possibly the major NAT involved in etamicastat *N*-acetylation; however, the contribution of NAT1 should not be excluded, because the enzymes involved will be dependent not only on the kinetics of the reaction, but also on the amount of compound that reaches the respective tissue and most significantly on the enzyme levels present in the tissues. NAT2 is expressed predominantly in liver, whereas NAT1 is ubiquitously expressed (Winter and Unadkat, 2005). Therefore, it cannot be excluded that NAT1-mediated acetylation may have a role in the metabolism of etamicastat in nonhepatic tissues.

In conclusion, these results indicate that NAT2 and, to a lesser extent, NAT1 contribute to etamicastat N-acetylation. Furthermore, the high interspecies and intraspecies differences in N-acetylation should be taken into consideration when evaluating the in vivo bioavailability of etamicastat.

Authorship Contributions

Participated in research design: Loureiro, Wright, Soares-da-Silva.

Conducted experiments: Loureiro, Fernandes-Lopes.

Performed data analysis: Loureiro, Bonifácio.

Wrote or contributed to the writing of the manuscript: Loureiro, Bonifácio, Soares-da-Silva.

References

Bonifácio MJ, Igreja B, Wright L, Soares-da-Silva P (2009) Kinetic studies on the inhibition of dopamine-β-hydroxylase by BIA 5-453 (Abstract). *pA2 Online* 7:050P.

Cascorbi I, Drakoulis N, Brockmöller J, Maurer A, Sperling K, and Roots I (1995) Arylamine N-acetyltransferase (NAT2) mutations and their allelic linkage in unrelated Caucasian individuals: correlation with phenotypic activity. *Am J Hum Genet* **57**:581–592.

Dorne JL (2004) Impact of inter-individual differences in drug metabolism and pharmacokinetics on safety evaluation. *Fundam Clin Pharmacol* **18**:609–620.

Estrada L, Kanelakis KC, Levy GN, and Weber WW (2000) Tissue- and gender-specific expression of N-acetyltransferase 2 (Nat2*) during development of the outbred mouse strain CD-1. *Drug Metab Dispos* **28**:139–146.

Gao W, Johnston JS, Miller DD, and Dalton JT (2006) Interspecies differences in pharmacokinetics and metabolism of S-3-(4-acetylamino-phenoxy)-2-hydroxy-2-methyl-N-(4-nitro-3-trifluoromethylphenyl)-propionamide: the role of N-acetyltransferase. *Drug Metab Dispos* **34**: 254–260.

Glinsukon T, Benjamin T, Grantham PH, Weisburger EK, and Roller PP (1975) Enzymic N-acetylation of 2,4-toluenediamine by liver cytosols from various species. *Xenobiotica* **5**: 475–483.

Grant DM, Blum M, Beer M, and Meyer UA (1991) Monomorphic and polymorphic human arylamine N-acetyltransferases: a comparison of liver isozymes and expressed products of two cloned genes. *Mol Pharmacol* **39**:184–191.

Hein DW, Doll MA, Fretland AJ, Leff MA, Webb SJ, Xiao GH, Devanaboyina US, Nangju NA, and Feng Y (2000a) Molecular genetics and epidemiology of the NAT1 and NAT2 acetylation polymorphisms. *Cancer Epidemiol Biomarkers Prev* **9**:29–42.

Hein DW, McQueen CA, Grant DM, Goodfellow GH, Kadlubar FF, and Weber WW (2000b) Pharmacogenetics of the arylamine N-acetyltransferases: a symposium in honor of Wendell W. Weber. *Drug Metab Dispos* **28**:1425–1432.

Husain A, Zhang X, Doll MA, States JC, Barker DF, and Hein DW (2007) Identification of N-acetyltransferase 2 (NAT2) transcription start sites and quantitation of NAT2-specific mRNA in human tissues. *Drug Metab Dispos* **35**:721–727.

Igreja B, Pires NM, Wright L, and Soares-da-Silva P (2008) Effect of combined administration of BIA 5-453 and captopril on blood pressure and heart rate (Abstract). *Hypertension* **52**:E62.

Igreja B, Pires NM, Wright LC, and Soares-da-Silva P (2011) Antihypertensive effects of a selective peripheral dopamine beta-hydroxylase inhibitor alone or in combination with other antihypertensive drugs [Abstract]. *Hypertension* **58**:E161–E162.

Levy GN, Martell KJ, DeLeon JH, and Weber WW (1992) Metabolic, molecular genetic and toxicological aspects of the acetylation polymorphism in inbred mice. *Pharmacogenetics* **2**: 197–206.

Mahmood I, Green MD, and Fisher JE (2003) Selection of the first-time dose in humans: comparison of different approaches based on interspecies scaling of clearance. *J Clin Pharmacol* **43**:692–697.

Meyer UA (1994) Polymorphism of human acetyltransferases. *Environ Health Perspect* **102** (**Suppl 6**):213–216.

Nunes T, Rocha JF, Vaz-da-Silva M, Falcão A, Almeida L, and Soares-da-Silva P (2011) Pharmacokinetics and tolerability of etamicastat following single and repeated administration in elderly versus young healthy male subjects: an open-label, single-center, parallel-group study. *Clin Ther* **33**:776–791.

Nunes T, Rocha JF, Vaz-da-Silva M, Igreja B, Wright LC, Falcão A, Almeida L, and Soares-da-Silva P (2010) Safety, tolerability, and pharmacokinetics of etamicastat, a novel dopamine-β-hydroxylase inhibitor, in a rising multiple-dose study in young healthy subjects. *Drugs R D* **10**:225–242.

Otsuka M, Furuuchi S, Usuki S, Nitta S, and Harigaya S (1983) Metabolism of afloqualone, a new centrally acting muscle relaxant, in monkeys and dogs. *J Pharmacobiodyn* **6**: 708–720.

Rocha JF, Vaz-da-Silva M, Nunes T, Igreja B, Loureiro AI, Bonifácio MJ, Wright LC, Falcão A, Almeida L, and Soares-da-Silva P (2011) Single-dose tolerability, pharmacokinetics, and pharmacodynamics of etamicastat (BIA 5-453), a new dopamine beta-hydroxylase inhibitor, in healthy subjects. *J Clin Pharmacol* **52**:156–170.

Savidge RD, Bui KH, Birmingham BK, Morse JL, and Spreen RC (1998) Metabolism and excretion of zafirlukast in dogs, rats, and mice. *Drug Metab Dispos* **26**:1069–1076.

Sharer JE, Shipley LA, Vandenbranden MR, Binkley SN, and Wrighton SA (1995) Comparisons of phase I and phase II in vitro hepatic enzyme activities of human, dog, rhesus monkey, and cynomolgus monkey. *Drug Metab Dispos* **23**:1231–1241.

Spielberg SP (1996) N-acetyltransferases: pharmacogenetics and clinical consequences of polymorphic drug metabolism. *J Pharmacokinet Biopharm* **24**:509–519.

Stanley LA and Sim E (2008) Update on the pharmacogenetics of NATs: structural considerations. *Pharmacogenomics* **9**:1673–1693.

Stevens GJ, Payton M, Sim E, and McQueen CA (1999) N-acetylation of the heterocyclic amine batracylin by human liver. *Drug Metab Dispos* **27**:966–971.

Sugamori KS, Wong S, Gaedigk A, Yu V, Abramovici H, Rozmahel R, and Grant DM (2003) Generation and functional characterization of arylamine N-acetyltransferase Nat1/Nat2 double-knockout mice. *Mol Pharmacol* **64**:170–179.

Vaz-da-Silva M, Nunes T, Rocha JF, Falcão A, Almeida L, and Soares-da-Silva P (2011) Effect of food on the pharmacokinetic profile of etamicastat (BIA 5-453). *Drugs R D* **11**:127–136.

Walraven JM, Trent JO, and Hein DW (2008) Structure-function analyses of single nucleotide polymorphisms in human N-acetyltransferase 1. *Drug Metab Rev* **40**:169–184.

Winter HR and Unadkat JD (2005) Identification of cytochrome P450 and arylamine N-acetyltransferase isoforms involved in sulfadiazine metabolism. *Drug Metab Dispos* **33**: 969–976.

Address correspondence to: P. Soares-da-Silva, Department of Research and Development, BIAL – Portela & C^a, S.A., À Av. da Siderurgia Nacional, 4745-457 S. Mamede do Coronado, Portugal. E-mail: psoares.silva@bial.com